ELSEVIER

International Journal of Mass Spectrometry 223–224 (2003) 459–471

International Journal of Mass Spectrometry

www.elsevier.com/locate/ijms

Selected ion flow tube study of NH_4^+ association and of product switching reactions with a series of organic molecules

Nigel G. Adams*, Lucia M. Babcock, Toufik M. Mostefaoui, Michael S. Kerns

Department of Chemistry, The University of Georgia, Athens, GA 30602, USA

Received 30 January 2002; accepted 24 May 2002

Abstract

A study has been made of the association reactions of NH_4^+ with a series of organic molecules, CH_3OH, C_2H_5OH, $(CH_3)_2O$, CH_3CHO, CH_3CO_2H and $(CH_3)_2CO$, at 300 K using a Selected Ion Flow Tube (SIFT). Ternary association rate coefficients have been determined and the product ions of several of the reactions have been probed by their further reactivities. The reaction with CH_3NH_2 was also studied, but this proceeds by proton transfer, being the only case in the study where this is energetically possible. The association reactions are generally rapid, and are pressure saturated in some cases, indicating strong bonding. Probing of the reactivity of the product ions of the $(CH_3)_2O$, CH_3CHO, CH_3CO_2H and $(CH_3)_2CO$ associations with the same set of molecules has shown that the reactions occur exclusively by switching, where one associated molecule is replaced by another. These switching reactions, when exothermic, can be very efficient, but the efficiency is strongly dependent on energetics. The study enabled both forward and reverse rate coefficients to be determined, and hence equilibrium constants, *K*, at 300 K; from these *K*'s relative bond energies were estimated. Relative bond energies for NH_4^+ bound to the neutral are $(CH_3)_2CO > CH_3CO_2H > CH_3CHO > (CH_3)_2O$, with the bond to $(CH_3)_2CO$ being substantially stronger than the others. The reaction mechanism is suggestive of a strong cluster bond, although a chemically reactive alternative is possible and is discussed. Interstellar implications are mentioned. (Int J Mass Spectrom 223–224 (2003) 459–471)

Keywords: SIFT; Ion–molecule reactions; Rate coefficients; Association; Switching reactions; Molecular ion structures

1. Introduction

Ternary (three body or collisionally stabilized) ion-neutral reactions

$$A^+ + B + M \rightarrow AB^+ + M \quad (1)$$

where M is a third body, have been studied for many years [1] both because of their fundamental significance as an independent reaction process [2] and also because of their application in high pressure ionized media such as planetary atmospheres [3]. The analogous process of radiative association

$$A^+ + B \rightarrow AB^+ + h\nu \quad (2)$$

has also been suggested as a mechanism for producing large molecular ions in a single step and is particularly significant for the low-pressure environment of diffuse and dense clouds in the interstellar medium [4]. Radiative association is difficult to study experimentally and almost always the ternary process has, together with theory [5], been used to provide information on the rate coefficients for this binary mechanism.

* Corresponding author. E-mail: adams@chem.uga.edu

1387-3806/02/$ – see front matter
PII S1387-3806(02)00932-6

In addition to determining rate coefficients for the ternary process, there is also a further point of great significance, i.e., whether the product ion is the cluster ion $A^+ \cdot B$ or a more strongly bonded AB^+ species. For simplicity, the association product will be written as AB^+ in cases where the structural form of the product is not known. This question has, however, been answered for some reactions. For example, a study of the ternary association reactions of CH_3^+ with CH_3OH and H_3O^+ with C_2H_4 has shown that the former reaction produces exclusively protonated dimethyl ether, $(CH_3)_2OH^+$, whereas the latter gives protonated ethanol, $C_2H_5OH_2^+$, and in neither case does the weakly bound cluster, $CH_3^+ \cdot CH_3OH$ or $H_3O^+ \cdot C_2H_4$, survive [6,7]. That this occurs is corroborated by detailed theoretical calculations concerning the potential surfaces, which are becoming available for an ever-increasing number of systems [8]. The association reactions of CH_3^+ and H_3O^+ are particularly important to chemistry in the interstellar medium, since these species are rapidly produced in primary reactions of C^+ and O^+ with the abundant H_2 [9] and do not react further very rapidly. H_3O^+ does not react significantly with H_2 since it is fully hydrogenated, however, this would not be expected for CH_3^+ and indeed this reacts, albeit, slowly by association yielding CH_5^+ [10]. NH_4^+ is also produced readily in the interstellar medium and is unreactive with H_2 [11]. It is with NH_4^+ association reactions that the present study is concerned; the reactions of CH_3^+ and H_3O^+ have been studied extensively previously [1,12]. The question addressed is whether NH_4^+ reacts by association and, if association occurs, whether the electrostatic cluster or a more strongly bonded molecular species is produced. Which product dominates depends of course on the form of the potential surface and the heights of the potential barriers at the transition states. In order to investigate this further and find possible routes to the N-containing species observed, and expected to be present, in the interstellar medium [13], the association reactions:

$$NH_4^+ + X + He \rightarrow NH_4X^+ + He \quad (3)$$

have been studied, where X is one of a series of the organic molecules: CH_3OH, C_2H_5OH, $(CH_3)_2O$, CH_3CHO, CH_3CO_2H and $(CH_3)_2CO$. To investigate the structural forms of the reaction product NH_4X^+, further binary switching reactions of the type:

$$NH_4X^+ + Y \rightarrow NH_4Y^+ + X \quad (4)$$

have been studied, with Y again being one of the above organic molecules. Other types of reaction channel, i.e., those resulting in fragmentation, were searched for, but were not observed.

2. Experimental

The Selected Ion Flow Tube (SIFT) technique has been described in detail previously [14–16] and will only be briefly outlined here. NH_4^+ ions were created in a high-pressure electron-impact ion source (~0.2–0.3 Torr) containing ammonia, via ionization of NH_3 and the subsequent ion–molecule reaction:

$$NH_3^+ + NH_3 \rightarrow NH_4^+ + NH_2^\bullet \quad (5)$$

These ions were extracted from the ion source, separated from other residual ions by mass selection and focused by an electrostatic lens through a 1 mm orifice into the flow tube. There they were constrained to flow with a helium carrier gas (by the action of a large Roots type blower pump) to an orifice, which is the entrance to a downstream mass spectrometer and ion detection system. Helium of purity 99.995% was further purified by passage through liquid nitrogen cooled molecular sieve and introduced into the flow tube at a rate of about 220 Torr L s^{-1} which established a pressure of about 0.5 Torr with an ion flow velocity, v_i, of $\sim 1.2 \times 10^4$ cm s^{-1} and a residence time in the flow tube of ~10 ms. In the studies of the NH_4^+ association reactions, reactant gases or vapors were introduced into the flow tube through one of a series of ring type injectors (typically 30, 60 and 85 cm upstream of the detection orifice) depending on the magnitude of the rate coefficient. Here the gas, along with a small flush of clean helium, was introduced in the upstream direction to produce rapid mixing;

the helium flush ensures that a steady state situation is rapidly achieved, even with sticky gases. Reactant flows were accurately determined by measuring the input pressure to—and pressure drop across—a calibrated capillary and using the Poiseuille equation. Rate coefficients were then determined in the conventional manner [16]. For the studies of the NH_4X^+ reactions, the gas, X, used to produce the association ion, was added upstream in sufficient concentration for the reaction to have proceeded close to completion, so that most of the NH_4^+ had reacted away by the time that the reactant gas, Y, was added at the downstream port. Reactant gases were used directly as supplied by the manufacturer and liquid samples were freeze–pump–thawed several times before use to eliminate gaseous impurities. The purities of the reactants as quoted by the manufacturers are as follows: CH_3OH (99.9 + wt.%), C_2H_5OH (200 proof), $(CH_3)_2O$ (99.87 mol%), CH_3CHO (99.4 wt.%), CH_3CO_2H (99.8 wt.%) and $(CH_3)_2CO$ (99.9 wt.%). All measurements were made at 300 K.

3. Results and data analysis

Analysis of the association reaction data, illustrated in Fig. 1a and b is straightforward and needs little explanation. The continuity equation for loss of the reactant ion by reaction (1) is

$$v_i \frac{\partial[A^+]}{\partial z} = -k[A^+][B] \quad (6)$$

where v_i is the average axial ion velocity in the flow tube, [ ] indicates the concentrations of the enclosed species and k is the effective binary rate coefficient which is equal to $k_{(3)}[M]$, where $k_{(3)}$ is the ternary (three body) rate coefficient and [M] is the concentration of the third body. The solution of Eq. (6) has the form [16],

$$[A^+]_z = [A^+]_0 \exp - \frac{k[B]z}{v_i} \quad (7)$$

Thus, $k_{(3)}$ can be obtained from plots such as those in Fig. 1 at a series of pressure of M and are listed in Table 1 together with the effective binary rate coefficients at 0.5 Torr. However, the situation for the switching reactions (e.g., reaction (4)) is more complex and requires some discussion. In studying the switching reactions of NH_4X^+ with Y, a complication in obtaining information about the structural form arises because these ionic species are not the only ions present in the flow tube. This is evident in Fig. 1b, which shows the variations of NH_4^+, NH_4X^+, and $NH_4X_2^+$ with X addition in the association reaction with C_2H_5OH. The figure shows the variation in ion concentration with X addition for a constant sampling

Table 1
Experimentally determined ternary rate coefficients, $k_{(3)}$, at 300 K for the reactions of NH_4^+ with the large organic molecules indicated

Reactant neutral	Effective binary k ($cm^3\ s^{-1}$)[a]	Theoretical k ($cm^3\ s^{-1}$)[b]	Reaction efficiency	Ternary $k_{(3)}$ ($cm^6\ s^{-1}$)
CH_3OH	2.2 (−11)	2.7 (−9)	8.2 (−3)	1.4 (−27)
C_2H_5OH	2.1 (−10)	2.7 (−9)	7.8 (−2)	1.2 (−26)
CH_3CHO	1.6 (−10)	3.8 (−9)	4.2 (−2)	9.8 (−27)
CH_3CO_2H	1.9 (−9)	2.7 (−9)	7.0 (−1)	≥1.2 (−25)
$(CH_3)_2CO$	8.6 (−10)	4.0 (−9)	2.2 (−1)	≥5.1 (−26)
$(CH_3)_2O$	2.2 (−10)	2.4 (−9)	9.2 (−2)	1.4 (−26)
CH_3NH_2[c]	1.4 (−9)	2.4 (−9)	5.8 (−1)	–

Effective binary rate coefficients, $k_{(3)}[M]$, are quoted at 0.5 Torr to allow direct comparison with the rate coefficients for the switching reactions.

[a] Value of the rate coefficient at 0.5 Torr.

[b] Collisional rate coefficients calculated using Variational Transition State Theory [17], using polarizabilities and dipole moments obtained from the literature [18,19].

[c] The product in this case is predominantly proton transfer, not association, and therefore there is no ternary rate coefficient.

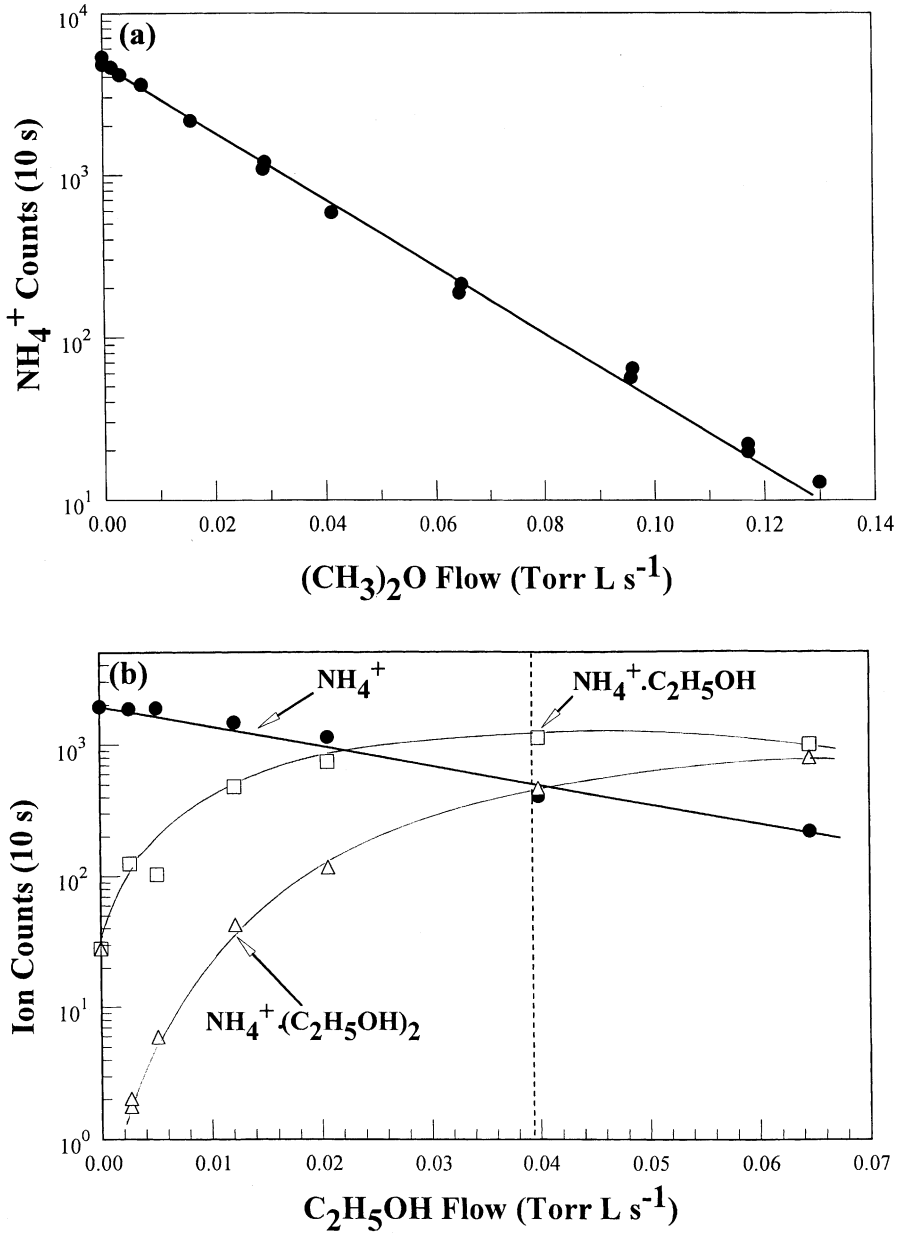

Fig. 1. Variation of the ion count rates for the association reactions of NH_4^+ with (a) $(CH_3)_2O$ and (b) C_2H_5OH. The former plot illustrates the linearity that can be obtained in the primary ion decay (greater than two orders of magnitude) whilst in the latter, both the primary and secondary ions are illustrated showing the sequential clustering. A correction has been made for mass discrimination against the higher mass ions.

position (i.e., the detection orifice), but it is also indicative of the variations in ion concentration as a function of distance along the flow tube for a constant concentration of X. Therefore at the position along the flow tube where Y is added, for the optimum situation an intermediate flow of X (as indicated by the vertical dashed line in Fig. 1b) is introduced upstream so that the NH_4X^+ concentration is dominant at the Y addition point, but with NH_4^+ and the $NH_4X_2^+$ secondary association ion from the reaction

$$NH_4X^+ + X + He \rightarrow NH_4X_2^+ + He \quad (8)$$

both being present in significant concentrations. Reactant X will also be present which could react with the ion products of the reaction with Y complicating the analysis. However, in all the cases studied, the reactions proceed by the simple mechanism of switching (i.e., no other types of products, such as fragmentation products were observed) as is illustrated in reaction (4), thus making the situation tractable. In addition, since the association reactions of NH_4^+ with X have already been studied, their effects can be accounted for in the analysis. Finally, reactions of the higher order complex, $NH_4X_2^+$, with Y produce higher order products, as indicated by the mass balance in the reactions and thus do not influence this analysis.

The situation is, then, that any residual NH_4^+ remaining in the flow tube after the addition point of Y can competitively associate with Y

$$NH_4^+ + Y + He \rightarrow NH_4Y^+ + He \quad (9)$$

to produce NH_4Y^+ which may or may not react with the source gas X in the flow tube by the switching reaction

$$NH_4Y^+ + X \rightarrow NH_4X^+ + Y \quad (10)$$

(the reverse of reaction (4)) depending on the energetics. The association reaction with Y to some extent competes with the NH_4^+ association with X causing a reduction in NH_4X^+ depending on the amount of NH_4^+ remaining at the Y addition point. The effect of the switching reaction will not be as complex as might originally be thought since, in the switching reactions, if NH_4Y^+ reacts rapidly with X (reaction (10)), then this is the exothermic direction and the endothermic reaction of NH_4X^+ with Y (reaction (4)) will not generally occur to any significant extent. However, there is also the possibility that the reaction is close to thermoneutral (i.e., the bond strengths of X and Y to NH_4^+ are similar) and this occurs in some of the data. For the present study, a series of situations need to be analyzed and are considered in Sections 3.1–3.3.

3.1. Switching reaction (4) exothermic: reactions (3), (4) and (9) dominant

This situation can be analyzed in a straightforward fashion from the kinetic equations for NH_4^+ and NH_4X^+ giving

$$[NH_4X^+] = C_1 \exp - (k_3[X] + k_9[Y])[He]z/v_i + C_2 \exp - k_4[Y]z/v_i \quad (11)$$

where C_1 and C_2 are constants, k is the rate coefficient with the subscript indicating the particular reaction equation, the square brackets represent the concentration of the enclosed species and z is the reaction distance with v_i being the ion velocity. Thus, the NH_4X^+ signal will decrease with the flow of Y in a double exponential fashion. This is illustrated in Fig. 2a for the reaction of $NH_4^+ \cdot CH_3CO_2H$ with C_2H_5OH, which fitting yields values for the rate coefficients k_4 and k_9. These rate coefficients and the constants C_1 and C_2 are the adjustable parameters in the fit. Since k_9 in the form of k_3 has already been measured in the NH_4^+ association reaction study (Table 1), k_4 can be identified immediately. When k_4 is large, it shows that this is the exothermic direction and thus for the reaction illustrated in Fig. 2a, that the bond of C_2H_5OH with NH_4^+ is stronger than that of CH_3CO_2H with NH_4^+. This pattern occurs frequently throughout the whole series of reactions and implies the existence of a strong cluster bonds. If that is the case, this observation is extremely significant to interstellar chemistry [20] since, unless rearrangement can occur on the much longer time scale of the interstellar medium (about 1 day between collisions with H_2) or in collision with H_2, such

associations may not be the source of the larger more complex interstellar molecules. Note that the observed interstellar species are generally neutral and thus a neutralization process such as electron–ion or ion–ion recombination must be involved. These processes are quite energetic [21,22] and may still be the mechanism by which isomerization to a more strongly bonded neutral form occurs. Alternatively, these species may

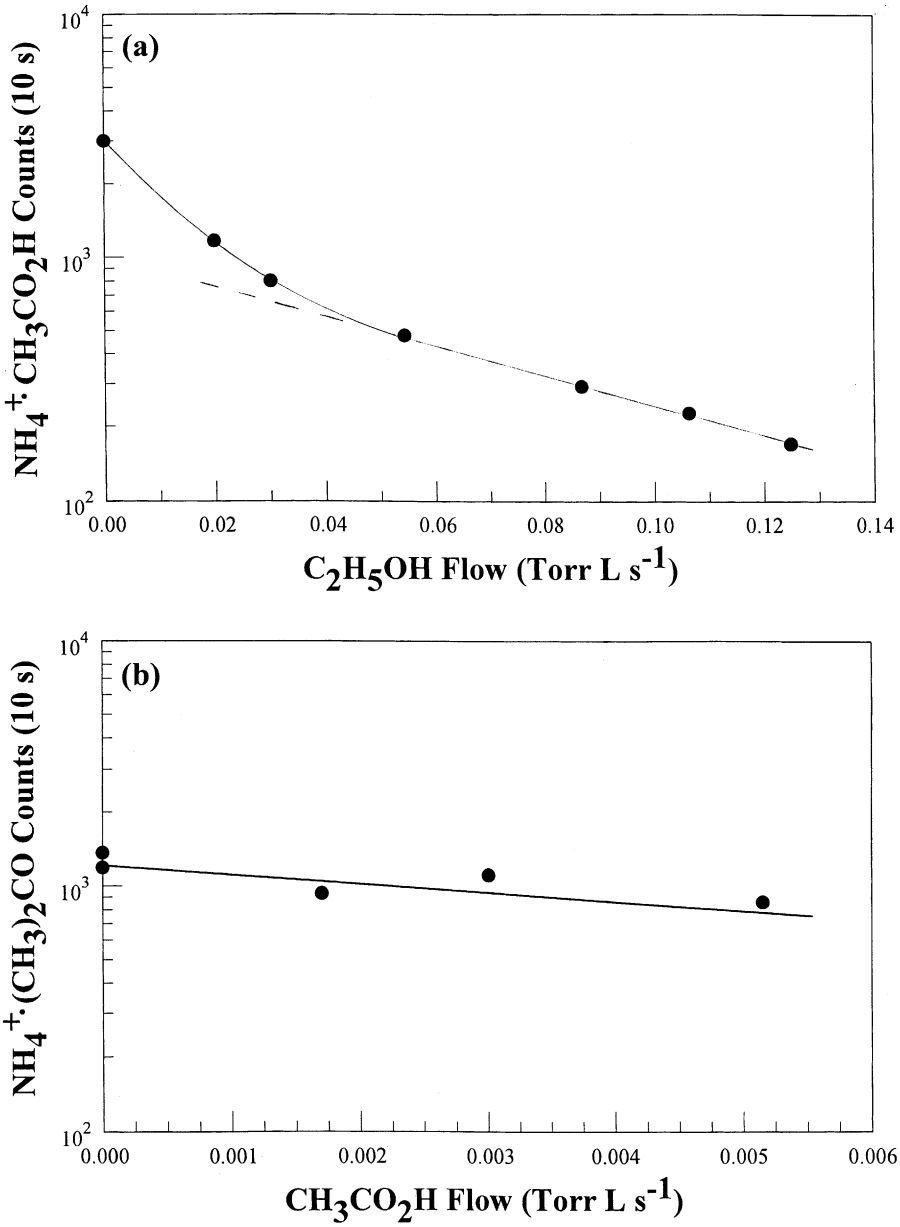

Fig. 2. Variation of the cluster ion, $NH_4^+ \cdot X$, count rates with neutral reactive gas flow to illustrate a series of types of behavior: (a) double exponential decay of $NH_4^+ \cdot CH_3CO_2H$ with C_2H_5OH addition, (b) negligible decay of $NH_4^+ \cdot (CH_3)_2CO$ with CH_3CO_2H addition, and (c) delayed decay of $NH_4^+ \cdot CH_3CO_2H$ with CH_3CHO addition. The dashed line in (a) is an extension of the linear decay to small flows to illustrate the additional exponential component in this region.

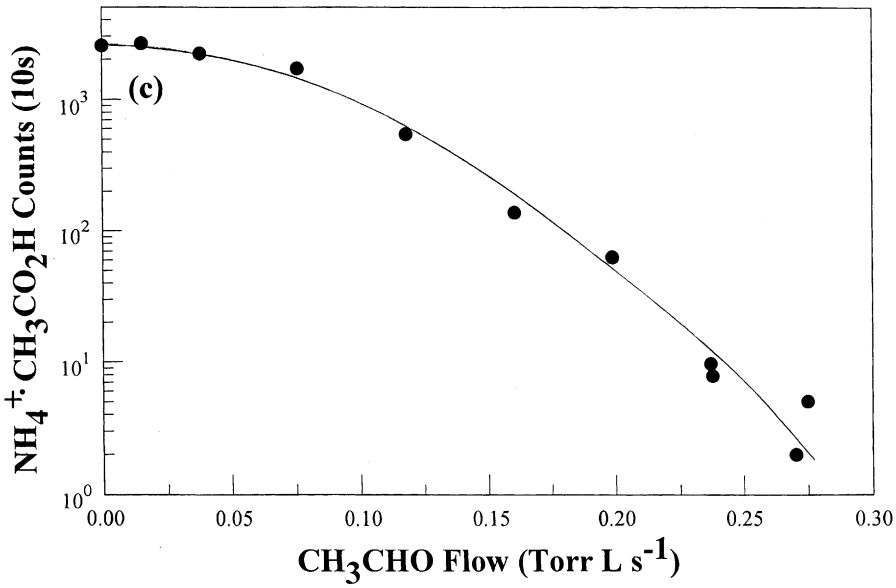

Fig. 2. (*Continued*).

just dissociate at the cluster bond, adding little to molecular evolution. Nothing is presently known about the products of cluster ion recombination [23]. Note that if the two body rate coefficients, k_4 and k_9 [He], are similar then a pseudo linear decay curve will be observed, as is seen in some cases.

3.2. Switching reaction (4) endothermic: reactions (3), (9) and (10) dominant

In the case where reaction (4) is endothermic, it will not contribute so significantly to the loss of NH_4X^+; however, then the reverse exothermic reaction (10) can occur. Thus as Y is added, it competes with X for NH_4^+. As soon as NH_4Y^+ is produced, reaction (10) converts it back to NH_4X^+ and there is essentially no reduction in the NH_4X^+ signal due to this. However, as Y is increased, eventually reaction (4) can start to compete with its reverse giving rise to a decay in the NH_4X^+ signal, and a value of the rate coefficient for reaction (4) is obtained. This is an extreme case of that discussed below in Section 3.3. This situation occurs for the reaction $NH_4^+ \cdot (CH_3)_2CO$ with CH_3CO_2H (see Fig. 2b) showing that the bond to $(CH_3)_2CO$ is stronger than that to CH_3CO_2H. Detailed information on the rate coefficient for the reverse exothermic reaction (10) can be obtained by studying the reaction.

$$NH_4^+ \cdot CH_3CO_2H + (CH_3)_2CO \rightarrow NH_4^+ \cdot (CH_3)_2CO + CH_3CO_2H \quad (12)$$

3.3. Forward and reverse switching reactions (4) and (10) close to thermoneutral: reactions (3), (4), (9) and (10) all occur

Yet another form of decay curve that was initially very surprising is illustrated in Fig. 2c for the reaction of $NH_4^+ \cdot CH_3CO_2H$ with CH_3CHO. Such behavior is possible when both reactions (4) and (10) can occur significantly, i.e., when the reaction is close to thermoneutral. In this situation, if the endo-/exo-thermicity is sufficiently small, both the forward and reverse rate coefficients will be appreciable and equilibrium may be achieved. The equilibrium constant, K, is given by:

$$K = \frac{k_4}{k_{10}} = \frac{[NH_4Y^+][X]}{[NH_4X^+][Y]}, \text{ i.e., } \frac{[NH_4Y^+]}{[NH_4X^+]} = \frac{K[Y]}{[X]} \quad (13)$$

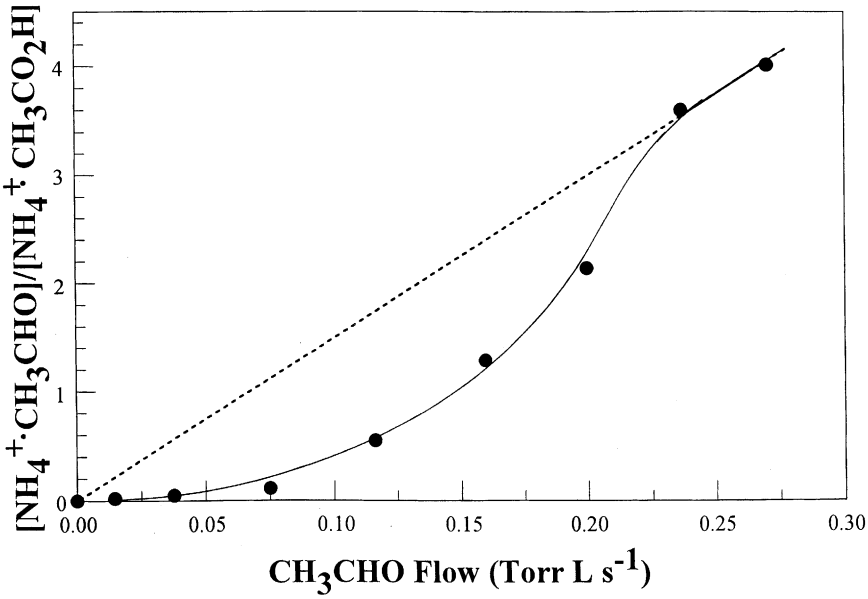

Fig. 3. A plot of $[NH_4^+ \cdot CH_3CHO]/[NH_4^+ \cdot CH_3CO_2H]$ vs. flow of CH_3CHO for the reaction of $NH_4^+ \cdot CH_3CO_2H$ with CH_3CHO. The data indicate the approach to equilibrium for flow less than 0.2 Torr L s^{-1} and the attainment of equilibrium for larger flows.

and thus a plot of the ratio of the ion signals vs. [Y] should yield a straight line of slope K/[X]. Such a plot is illustrated in Fig. 3 for the data in Fig. 2c. The lack of linearity at low flows of Y indicates that equilibrium is not achieved until flows $\geq$0.2 Torr L s^{-1}. Thus, the form of the decay curve in Fig. 2c can now be explained. As the flow of Y is increased, association with Y competes with that of X, but the larger concentration of X converts NH_4Y^+ back to NH_4X^+ giving no significant decrease in the primary ion. As the flow of Y becomes larger, the switching reaction to regenerate NH_4X^+ can no longer compete and its signal level decreases both due to the association reaction (9) and the switching reaction (4), until at higher flows, equilibrium is approached. Here the NH_4X^+ signal will still decrease with increasing Y because of the shift in the equilibrium. From all of these data for the reaction of $NH_4^+ \cdot CH_3CO_2H$ with CH_3CHO, with an analysis of the approach to equilibrium [24], approximate values of k_4 and k_{10} (see Table 2) and a K of 0.38 have been deduced showing that $k_{10} > k_4$. Such results indicate that these bonds are of similar strength with the equilibrium constant giving the enthalpy difference, ΔH, in the reaction [25],

$$\Delta H - T\Delta S = -RT \ln K \quad (14)$$

i.e., the difference in the bond strengths, if the entropy difference, ΔS, can be determined. In fact for such a situation, ΔS is expected to be close to zero. Based on all of the above deliberations, the complete data set has been used to determine the rate coefficients of the switching reactions and the relative bond strengths to NH_4^+.

Which type of behavior, discussed in Sections 3.1–3.3, occurs in specific cases depends on the magnitudes of the rate coefficients, k_3, k_4, k_9 and k_{10}, the concentration of X and the range of concentrations of Y. The magnitudes of some of the effects will also be dependent on how large the NH_4^+ concentration is in relation to NH_4X^+ (a factor of 0.36 for the data illustrated in Fig. 1b). As can be seen in Table 2, a wide range of rate coefficients is evident in the data presented here.

Table 2
Experimentally determined binary rate coefficients for the reactions of the NH_4^+ clusters, NH_4X^+, indicated with the organic molecules, Y, shown

Reactant neutral	Rate coefficient ($cm^3\,s^{-1}$)				
	$NH_4^+\cdot CH_3CHO$	$NH_4^+\cdot CH_3CO_2H$	$NH_4^+\cdot(CH_3)_2O$	$NH_4^+\cdot(CH_3)_2CO$	Theoretical[a]
CH_3OH	8.8 (−11)	2.2 (−13)	2.2 (−13)	9.4 (−11)	2.0 (−9)
C_2H_5OH	8.5 (−10)	7.3 (−11)	–[b]	2.9 (−10)	1.9 (−9)
CH_3CHO	–[c]	∼4 (−10)	3.6 (−10)	≤1 (−13)	2.6 (−9)
CH_3CO_2H	∼1 (−9)	–[c]	7.5 (−10)	≤1 (−13)	1.8 (−9)
$(CH_3)_2O$	6.6 (−11)	3.5 (−11)	–[c]	≤1 (−13)	1.7 (−9)
$(CH_3)_2CO$	5.1 (−9)	2.6 (−9)	2.6 (−9)	–[c]	2.6 (−9)
CH_3NH_2[d]	1.4 (−9)	1.7 (−9)	1.5 (−9)	1.3 (−9)	1.8 (−9)

This gives forward and reverse rate coefficients for the individual switching reactions enabling equilibrium constants to be determined. In some cases the reverse rate coefficient was too small to be measured accurately and only an upper limit can be given.

[a] Collisional rate coefficients calculated from Variational Transition State Theory [17], using polarizabilities and dipole moments obtained from the literature [18,19].

[b] Reactions involving X and Y which are isomeric forms could not be studied because the reactant and product masses are identical.

[c] Symmetrical reactions, i.e., with X and Y identical, could not be studied.

[d] The reaction product was predominantly proton transfer.

4. Discussion

Rate coefficients for the association reactions are presented in Table 1, both in the form of effective binary rate coefficients at 0.5 Torr (for comparison with those for the switching reactions) and as ternary rate coefficients. Note that when the effective binary rate coefficient is large, the reaction is pressure saturated [24], i.e., independent of the He pressure, and in these cases only a lower limit to the ternary rate coefficient can be obtained. Also included in Table 1 are the collisional rate coefficients determined using variational transition state theory [17] with polarizabilities and dipole moments being taken from the literature [18,19]. Note that the effective binary rate coefficients and thus the efficiency of the reactions are quite large. When the efficiency approaches 1, as in the cases of the NH_4^+ associations with CH_3CO_2H and $(CH_3)_2CO$, this indicates that the ternary reaction is close to saturation. The standard reaction mechanism for ternary reactions of the type in reaction (1) is

$$A^+ + B \underset{k^-}{\overset{k^+}{\rightleftharpoons}} AB^{+*} \xrightarrow{M} AB^+ + M^* \qquad (15)$$

This indicates that, in these cases, the intermediate AB^{+*} is stabilized by M on almost every association of A^+ with B. Thus, only an upper limit to the ternary rate coefficient, $k_{(3)}$ can be obtained. The high efficiency of these reactions most likely due to the long lifetime of the intermediate AB^{+*} against unimolecular decomposition (i.e., k^- small relative to the stabilization rate) for these very polyatomic intermediates (13 and 15 atoms), which varies with complexity [26]. It is also indicative that these $A–B^+$ bonds are strong [26], as confirmed later in Table 3. The $k_{(3)}$ also indicate that the $A–B^+$ bonds in the other complexes are also strong (but not as strong as in the two cases above). Thus, these reactions are not close to pressure saturation (i.e., the effective binary rate coefficients are not independent of the concentration of M) and values of the $k_{(3)}$ can be obtained.

Table 3
Bond strengths relative to $(CH_3)_2O$ for clusters to NH_4^+

Clusteredspecies	Relative bond strength (kcal mol^{-1})	Proton affinities (kcal mol^{-1})
$(CH_3)_2CO$	≥7.7	194
CH_3CO_2H	1.7	187.3
CH_3CHO	1.0	183.7
$(CH_3)_2O$	0	189.0

The values are listed in order of decreasing bond strength. The limit for $(CH_3)_2CO$ occurs because of the limits on K in Table 4. Also included are the proton affinities [27] of the clustered ligands.

The above data are extremely useful for determining which rate coefficient in the double exponential data corresponds to association and which to switching. By these means, and as considered in Section 3, the rate coefficients for the switching reactions were determined and are given in Table 2. It is not possible to obtain all combinations of X and Y, since for those situations where species are identical or structural isomers, the masses of the reactant and product ions are identical and thus are mass spectrometrically indistinguishable. However, in the majority of the cases, rate coefficients or limits for both the exo- and endo-thermic directions could be obtained. The data show that there are appreciable differences in the rate coefficients for the various systems indicating significant differences in the strengths of the bonds to NH_4^+. Comparison of these data with the collision rate coefficients deduced from variational transition state theory [17], indicates that when exothermic these reactions are quite efficient, approaching half of the collisional rate coefficient. The exception is reactions with $(CH_3)_2CO$, which are extremely efficient; this has the strongest bond to NH_4^+. Note that for the $NH_4^+{\cdot}CH_3CO_2H$ reaction with CH_3CHO, illustrated in Figs. 2c and 3, the rate coefficients are only approximate because of the approach to equilibrium. All of the rate coefficients were used to deduce the equilibrium constants or limits on equilibrium constants as given in Table 4.

Following this, the enthalpy changes in the reactions were determined using Eq. (14), and from these the relative bond strengths listed in Table 3 were estimated. This clearly shows that the bond to $(CH_3)_2CO$ is substantially stronger than that to CH_3CO_2H or CH_3CHO. These latter two are quite similar, with that to $(CH_3)_2O$ being somewhat weaker. This is not unreasonable if the ions are in the form of clusters. For the $(CH_3)_2C{=}O$, cluster, the O-atom will be the most electronegative due both to the double bond [28] and the negative charge donated by the two electron rich CH_3 groups [29]. Thus, there will be strong electrostatic bonding between the O-atom and the NH_4^+. For CH_3CO_2H and CH_3CHO, the electrostatic bonding is expected to be weaker since there is only one electron rich CH_3 group to donate negative charge to the doubly bonded O-atom. Thus as observed in Table 3, the strength of the bonds to NH_4^+ would be expected to be similar, with that to CH_3CO_2H being slightly stronger due to the slightly larger electron donation power of the OH grouping relative to the H-atom in CH_3CHO. The bonding to $(CH_3)_2O$ is the weakest in spite of the electron donating power of the two CH_3 groups, which is presumably due to the negation of this effect by the absence of the electron withdrawing effect of a double bond to O and perhaps the steric hindrance of the NH_4^+ by the CH_3 groups. Note that C_2H_5OH bonds more strongly than CH_3CO_2H (mentioned earlier). This shows the electron donating power of C_2H_5 with somewhat less steric hindrance than for $(CH_3)_2O$, due to the lesser size of the CH_2 group in the C_2H_5 relative to a CH_3 group. In the case of the other compounds, the presence of the C=O bonds to the electronegative

Table 4
Equilibrium constants, *K*, for the reactions of the NH_4^+ clusters, NH_4X^+, with the organic molecules, Y, as deduced from the data given in Table 2

	Equilibrium constants, *K*			
	$NH_4^+{\cdot}CH_3CHO$	$NH_4^+{\cdot}CH_3CO_2H$	$NH_4^+{\cdot}(CH_3)_2O$	$NH_4^+{\cdot}(CH_3)_2CO$
CH_3CHO	–[a]	∼3.8 (−1)	**5.45**	≤1.96 (−5)
CH_3CO_2H	∼**2.77**	–[a]	**2.14 (1)**	≤3.85 (−5)
$(CH_3)_2O$	1.83 (−1)	4.67 (−2)	–[a]	3.85 (−5)
$(CH_3)_2CO$	≥**5.1 (4)**	≥**2.6 (4)**	≥**2.6 (4)**	–[a]

The values in bold are for the exothermic direction of the reaction. Where only a limit on a rate coefficient is given in Table 2, only a limit can be given on the corresponding equilibrium coefficient.

[a] Symmetrical reactions, i.e., with X and Y identical, could not be studied.

O-atom make it much more exposed to the NH_4^+. A good indication of the relative strengths of the electrostatic bonds between the NH_4^+ and the neutral molecules should be the proton affinities of those molecules, although the equilibrium inter-particle separations may be different for NH_4^+ and H^+ and any steric hindrance effects will be much smaller for H^+. The proton affinities are given in Table 3 for comparison with the relative bond strengths determined in the present study. The interdependence of these parameters is shown in Fig. 4. Since a monotonic dependence would be expected (as is observed for the C=O containing species), this points to the proton affinity of $(CH_3)_2O$ being an inappropriately large value to use, due (as discussed earlier) to steric hindrance.

Although the occurrence of switching reactions and the above discussion implies strong cluster bonds, some caution is required in interpreting the data too readily in this way. This can be appreciated by examining the results for other association reactions that have been analyzed in detail such as those reviewed by Adams and Fisher [8]. For the association of CH_3^+ with H_2O and CH_3OH, protonated methanol, $CH_3OH_2^+$, and protonated dimethyl ether, $(CH_3)_2OH^+$, respectively, are known to be formed. That this occurs is not unreasonable, since the negatively charged O-atom would be attracted towards the positively charged CH_3^+ exactly where bonding takes place, a behavior consistent with theoretically calculated isomer energies and transition states for these systems.

That chemical bonding would also occur in the association of H_3O^+ with C_2H_4 is not so obvious. In this case, protonated ethanol, $C_2H_5OH_2^+$, is produced and here the ion is fully saturated whereas the neutral, possessing a double bond, is not. The reaction is considered to occur with the H_3O^+ attacking the C=C double bond with the H^+ migrating to one C-atom and the H_2O to the other. Thus, unlike the CH_3^+ reactions, there is bond breaking as well as making. Following this precedent, a mechanism for the NH_4^+ associations can be conceived. For the species, CH_3CO_2H, $(CH_3)_2CO$ and CH_3CHO, there is the O-atom doubly bonded to the central carbon.

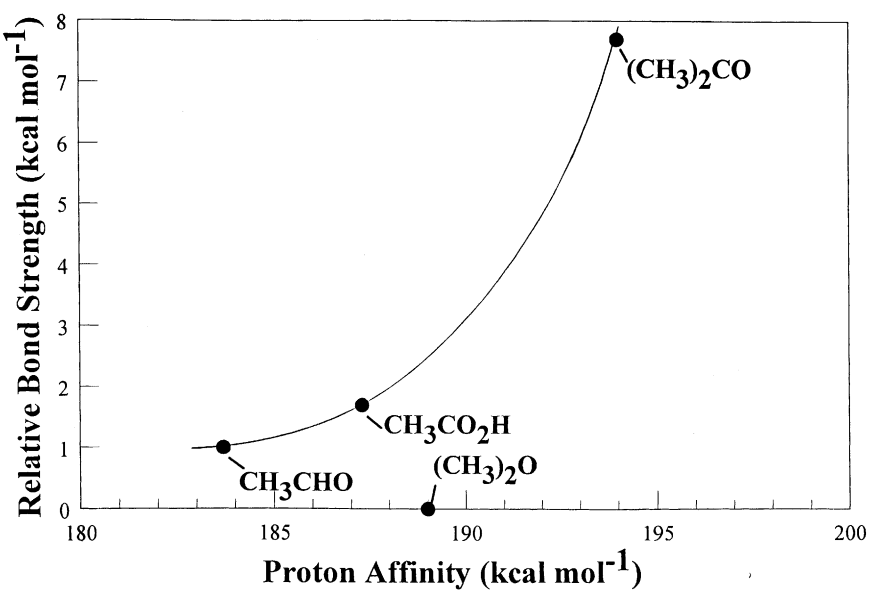

Fig. 4. Plot of the data in Table 3 as relative bond strength vs. proton affinity. Note that this is not linear indicating that there is not a one-to-one correspondence between the proton and NH_4^+ affinities; but note also that the curve in monotonic, as expected. The $(CH_3)_2O$ point is well off this curve, indicating that the proton affinity is not the appropriate value to use in this case due to steric hindrance or lack of chemical reactivity (see text).

Since this O-atom is electron rich, the NH_4^+ will have a propensity to move to this site (as discussed above). Thus, with the breaking of one of the bonds in the double bond, an H-atom can migrate to the carbon, which is its vicinity with the NH_3^+ remaining to bond to the O-atom. If such a rearrangement occurs, then during the switching reactions, the reverse would have to happen with the intermediate complex moving through an NH_4^+ bound dimer, before a similar, but reverse, process occurs in the product ion. That the switching reaction can be fairly efficient does not obviate this process, since the intermediates are likely to be long lived allowing the mechanism to occur with high probability. Thus in these cases, the association ion would not necessarily have to be in the form of a clustered species. If this is the mechanism, the association ions would have the form: CH_3CH_2–O–NH_3^+, CH_3(HO)CH–O–NH_3^+ and $(CH_3)_2$CH–O–NH_3^+ for acetaldehyde, acetic acid and acetone, respectively, and would be more strongly bonded. Other possibilities also exist such as NH_2 migrating to the C and H_2^+ to the O. For association with $(CH_3)_2O$, both of the reacting species are fully saturated and thus chemical bonding is unlikely. This would only allow electrostatic bonding in this situation, making the inter-particle bond strength less than in the other cases.

5. Conclusions

The relative NH_4^+ affinities have been determined for the associated complexes of NH_4^+ with $(CH_3)_2O$, CH_3CHO, CH_3CO_2H and $(CH_3)_2CO$. These studies have prompted a discussion of the structures of the associated ions in terms of electrostatic interactions and chemical bonding. By either mechanism, the $(CH_3)_2O$ associated ion behaves differently due to the fact that there is no C=O double bond, which could result in steric hindrance, and/or in lack of chemical reactivity. With the present data for the C=O containing species, it is not possible to distinguish between these two mechanisms. More extensive experimental studies are required with species for which only either chemical reactivity or steric hindrance is possible, and theoretical structure calculations need to be made, in order to identify the precise mechanism.

In addition to the fundamental significance, this distinction is important to the chemistry of interstellar gas clouds [4]. NH_4^+ is an important terminating ion in these media since it is unreactive with H_2 and is thus available to react with other species. The present study has shown that NH_4^+ associations are gas kinetic at the low temperatures of these clouds and thus that the production of NH_4^+ complexes will be efficient. If chemical reaction occurs rather than the formation of an electrostatically bonded complex, this would be a route to larger interstellar species. Otherwise, the electrostatically bonded complex, on electron–ion recombination, is likely to break up to give NH_3, H and the ligand, which will not advance the chemistry in these regions.

Acknowledgements

Financial support of NASA, Division of Planetary Sciences (Grant NAG5-8951) is gratefully acknowledged.

References

[1] Y. Ikezoe, S. Matsuoka, M. Takabe, A. Viggiano, Gas Phase Ion Molecule Reaction Rates through 1986, Maruzen, Tokyo, 1987.
[2] N.G. Adams, D. Smith, in: A. Fontijn, M.A.A. Clyne (Eds.), Reactions of Small Transient Species, Academic Press, London, 1983, p. 311.
[3] E.E. Ferguson, F.C. Fehsenfeld, D.L. Albritton, in: M.T. Bowers (Ed.), Gas Phase Ion Chemistry, vol. 1, Academic Press, New York, 1979, p. 45.
[4] E. Herbst, Adv. Gas Phase Ion Chem. 3 (1998) 1.
[5] D.R. Bates, E. Herbst, in: T.J. Millar, D.A. Williams (Eds.), Rate Coefficients in Astrochemistry, Kluwer, Dordrecht, 1988, p. 41.
[6] K.K. Matthews, N.G. Adams, N.D. Fisher, J. Phys. Chem. 101 (1997) 2841.
[7] K.K. Matthews, N.G. Adams, N.D. Fisher, Int. J. Mass Spectrom. Ion Proc. 163 (1997) 221.
[8] N.G. Adams, N.D. Fisher, Adv. Gas Phase Ion Chem. 3 (1998) 81.

[9] D. Smith, N.G. Adams, E.E. Ferguson, in: T.W. Hartquist (Ed.), Molecular Astrophysics, Cambridge University Press, Cambridge, 1990, p. 181.
[10] D. Smith, N.G. Adams, Chem. Phys. Lett. 54 (1978) 535.
[11] N.G. Adams, D. Smith, J.F. Paulson, J. Chem. Phys. 72 (1980) 288.
[12] V.G. Anicich, J. Phys. Chem. Ref. Data 22 (1993) 1469.
[13] M.C. McCarthy, in: A. Mezzacappa (Ed.), Stellar Evolution, Stellar Explosions and Galactic Chemical Evolution, IOP, Philadelphia, 1998, p. 205.
[14] N.G. Adams, D. Smith, Int. J. Mass Spectrom. Ion Phys. 21 (1976) 349.
[15] N.G. Adams, D. Smith, J. Phys. B 9 (1976) 1439.
[16] N.G. Adams, D. Smith, in: J.M. Farrar, W.H. Saunders (Eds.), Techniques for the Study of Ion-Molecule Reactions, Wiley, New York, 1988, p. 165.
[17] T. Su, W.J. Chesnavich, J. Chem. Phys. 76 (1982) 5183.
[18] D.R. Lide (Ed.), CRC Handbook of Chemistry and Physics, 78th ed., CRC, Boca Raton, FL, 1997.
[19] J.A. Dean (Ed.), Lange's Handbook of Chemistry, 14th ed., McGraw-Hill, New York, 1992.
[20] M.S. Kerns, N.D. Fisher, N.G. Adams, in: A. Mezzacappa (Ed.), Stellar Evolution, Stellar Explosions and Galactic Chemical Evolution, IOP, Philadelphia, 1998, p. 215.
[21] N.G. Adams, Adv. Gas Phase Ion Chem. 1 (1992) 271.
[22] N.G. Adams, Int. J. Mass Spectrom. Ion Proc. 132 (1994) 1.
[23] J.B.A. Mitchell, M. Larsson, I. Schneider (Eds.), Dissociative Recombination. IV. Theory, Experiments and Applications, World Scientific, Singapore, 1999.
[24] N.G. Adams, D.K. Bohme, D.B. Dunkin, F.C. Fehsenfeld, E.E. Ferguson, J. Chem. Phys. 52 (1970) 3133.
[25] I.M. Klotz, R.M. Rosenberg, Chemical Thermodynamics, 5th ed., Wiley, New York, 1994.
[26] H.S. Johnston, Gas Phase Reaction Rate Theory, The Ronald Press Co., New York, 1966.
[27] NIST Chemistry WebBook, NIST Standard Database 69, July 2001, http://webbook.nist.gov/chemistry/.
[28] J.B. Hendrickson, D.J. Cram, G.S. Hammond, Organic Chemistry, 3rd ed., McGraw-Hill, New York, 1970.
[29] R.T. Morrison, R.N. Boyd, Organic Chemistry, 2nd ed., Allyn and Bacon, Boston, 1971.